

# Magic numbers in copper-doped aluminum cluster anions

Owen C. Thomas, Weijun Zheng, and Kit H. Bowen, Jr.<sup>a)</sup>

*Department of Chemistry, Johns Hopkins University, Baltimore, Maryland 21218*

(Received 21 November 2000; accepted 26 December 2000)

Copper-doped aluminum cluster anions,  $\text{CuAl}_n^-$  were generated in a laser vaporization source and examined via mass spectrometry ( $n=2-30$ ) and anion photoelectron spectroscopy ( $n=2-15$ ). The mass spectrum of the  $\text{CuAl}_n^-$  series is dominated by  $\text{CuAl}_{13}^-$  with other magic numbers also appearing at  $n=6, 19,$  and  $23$ . The electron affinity versus cluster size trend shows a peak at  $n=6$  and a dip at  $n=13$ . These results are discussed in terms of the reordering of shell model energy levels and the enhanced stability of neutral  $\text{CuAl}_{13}$ . Reordering, which is a consequence of the copper atom residing in the central region of these clusters, provides an anion-oriented electronic rationale for the observed magic numbers. © 2001 American Institute of Physics.  
[DOI: 10.1063/1.1349547]

## INTRODUCTION

The discovery of fullerenes<sup>1</sup> and metcars<sup>2</sup> has inspired theorists to consider other unusually stable aggregates (magic clusters) that might serve as building blocks for cluster-assembled materials. If such exotic materials could be formed, they might well exhibit unique electronic, magnetic, optical, mechanical, and/or catalytic properties, and these could potentially lead to technological uses. While several types of magic clusters have now been considered by theory, doped aluminum clusters recur repeatedly as especially promising candidates. These fall into two relatively distinct categories,  $\text{Al}_n\text{X}$ , where X is a dopant such as B, Ga, C, Si, Ge, Ti, or As, and  $\text{MAl}_n$ , where M is an alkali metal atom. Several calculations have considered 13 atom,  $\text{Al}_{12}\text{X}$  clusters with icosahedral structures and the X atom at the center.<sup>3-8</sup> When X is a tetravalent atom,  $\text{Al}_{12}\text{X}$  clusters, with their 40 valence electrons, become closed electronic shell species, adding electronic stability to the geometric stability of their icosahedral structures. For example, calculations on  $\text{Al}_{12}\text{C}$  clusters found them to be carbon-centered icosahedra of high stability and inertness, suggesting that they would form a van der Waals-like solid in the bulk. Calculations on alkali-containing  $\text{MAl}_{13}$  clusters, on the other hand, told a different story, implying that these would form an extended ionic solid in the bulk.<sup>9-10</sup> The ionic nature of  $\text{MAl}_{13}$  depends on the fact that  $\text{Al}_{13}^-$  is itself a magic cluster which mimicks the electronic behavior of an atomic halogen anion.  $\text{Al}_{13}^-$  possesses electronic stability because it is a 40 valence electron, closed shell species; it has geometrical stability because it is an icosahedron, and it mimicks a halogen anion in that the electron affinity of  $\text{Al}_{13}$  is close to that of chlorine.<sup>11-15</sup> Calculations suggest that  $\text{KAl}_{13}$  clusters are best described as  $\text{K}^+\text{Al}_{13}^-$  “molecules”, analogous to alkali halide salts. In this case, the dopant alkali atomic ion sits outside the aluminum icosahedron, while in the case of the  $\text{Al}_{12}\text{X}$  clusters previously mentioned, the dopant resides inside the icosahedral cage.

In the present paper, we investigate the nature of copper-doped aluminum clusters,  $\text{CuAl}_n$  and their anions. Although copper atoms have similarities with alkali atoms that might be expected to put  $\text{CuAl}_n$  clusters in the same category with  $\text{MAl}_n$  clusters, they also have substantial differences, and these could put  $\text{CuAl}_n$  clusters in the other broadly-defined category, in which the dopant atom is endohedral among the aluminum atoms of the cluster. Chief among their similarities are the facts that both copper and alkali atoms have  $s^1$  valence electronic configurations, and that they exhibit monovalency in their homogeneous clusters.<sup>16-17</sup> Prominent among their differences, on the other hand, are the facts that copper atoms are much less electropositive than alkali atoms, and because of their  $d$  electrons, copper atoms exhibit a significantly higher ionization potential than the alkali metals, e.g.,  $\text{IP}(\text{Cu})-\text{IP}(\text{K})=3.4$  eV. To help characterize  $\text{CuAl}_n$  clusters and their anions, we have recorded the mass spectra of the  $\text{CuAl}_n^-$  homologous series and the negative ion photoelectron spectra of  $\text{CuAl}_n^-$ ,  $n=2-15$ . We have also drawn upon the recent theoretical calculations of Khanna and co-workers<sup>18</sup> on  $\text{CuAl}_n$  and  $\text{CuAl}_n^-$ .

## EXPERIMENT

Negative ion photoelectron spectroscopy is conducted by crossing a mass-selected beam of anions with a fixed-frequency photon source and energy analyzing the resultant photodetached electrons. This technique is governed by the following energy-conserving relationship,

$$h\nu = \text{EKE} + \text{EBE}, \quad (1)$$

where  $h\nu$  is the photon energy, EKE is the measured electron kinetic energy, and EBE is the electron binding energy.

In the present experiments, both mass spectra and the anion photoelectron (photodetachment) spectra were collected on an apparatus consisting of a laser vaporization source, a linear time-of-flight mass spectrometer for mass analysis and mass selection, and a magnetic bottle photoelectron spectrometer for electron energy analysis. The ion source consists of a Smalley-style laser vaporization source which utilizes a pulsed gas valve, a rotating and translating

<sup>a)</sup>Author to whom all correspondence should be addressed. Electronic mail: kitbowen@jhunix.hcf.jhu.edu

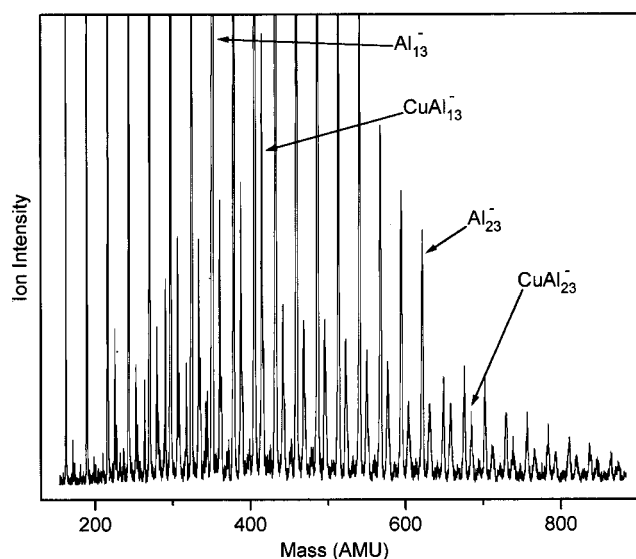


FIG. 1. Typical negative ion mass spectrum resulting from the use of a copper/aluminum alloy target rod in our laser vaporization source.

sample rod made of an aluminum/copper alloy (2011 aluminum, which is  $\sim 5\%$  copper), and second harmonic light pulses from a Nd:YAG laser. The cluster anions of interest were generated under two sets of source conditions, one utilizing essentially no helium in its expansion and the other using a larger internal volume laser vaporization block and  $\sim 4$  atm of helium gas behind its pulsed valve. In both cases, the source was aimed perpendicularly into the Wiley–McLaren extraction region of our time-of-flight mass spectrometer. Deflectors and an Einzel lens were positioned immediately downstream of the extraction plates. Just before the anions passed through the ion–photon interaction region, they encountered a mass gate followed by a momentum decelerator. Immediately after the ion–photon interaction region, a Channeltron electron multiplier monitored the arrival of the ions. At the ion–photon interaction region, electrons were photodetached from the anion of interest with the third harmonic of a second Nd:YAG laser. Most of these electrons were then energy analyzed by a magnetic bottle photoelectron spectrometer and detected with a multichannel plate. A LeCroy digital oscilloscope collected the data which was manipulated with a laboratory computer. The usual resolution of our magnetic bottle electron spectrometer during these experiments was  $\sim 50$  meV at an electron kinetic energy of  $\sim 1$  eV.

## RESULTS

### Mass spectra

Figure 1 shows a typical mass spectrum resulting from this work. Figure 2 shows the same mass spectrum with the component mass spectra of the  $\text{CuAl}_n^-$  homologous series and the  $\text{Al}_n^-$  homologous series separated from one another in Figs. 2(a) and 2(b), respectively. The intensities of the strongest peak in each spectrum have been normalized to the same value for ease of comparison. The mass spectrum in Fig. 2(a) is dominated by  $\text{CuAl}_{13}^-$ . This abundance pattern is

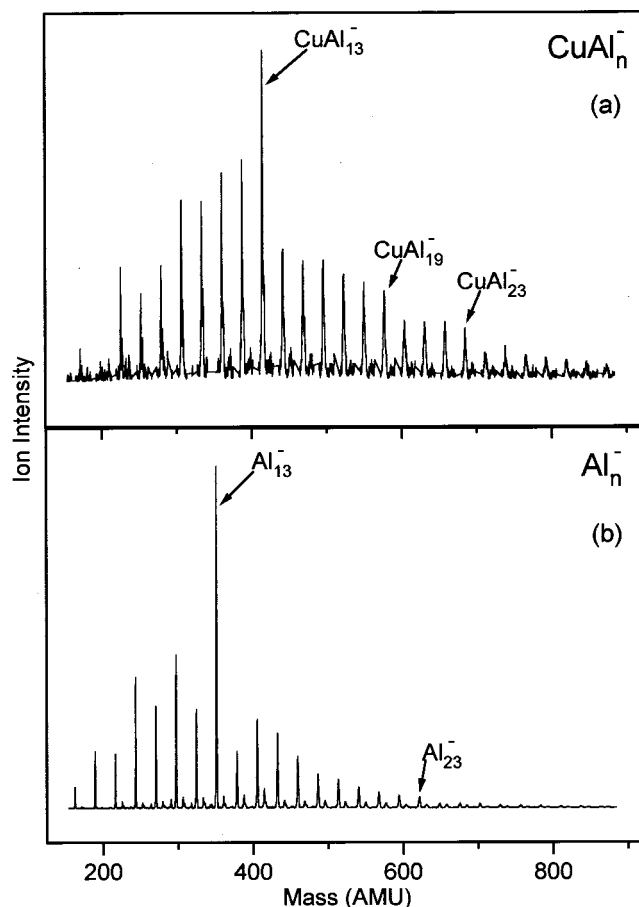


FIG. 2. This is the same mass spectrum as that shown in Fig. 1 but with the component mass spectra of the  $\text{CuAl}_n^-$  homologous series and the  $\text{Al}_n^-$  homologous series separated from one another in (a) and (b), respectively. The intensities of the strongest peak in each spectrum have been normalized to the same value for ease of comparison, i.e., (a) has been magnified by a factor of 17 relative to (b).

persistent from day to day, and it is easily the most striking single result of this work. The mass spectral abundance pattern shown here is typical of those taken without helium in the source. When helium gas was used, the ion intensities were substantially lower, but the resulting mass spectrum was still dominated by  $\text{CuAl}_{13}^-$ , albeit less dramatically so.

It is quite unexpected for a 41 valence electron cluster ion made up of atoms of free electron metals to be prominent in mass spectra. Usually, cluster species with one electron more than the number needed to form a closed electronic shell show a local intensity minimum (a dip) in their mass spectra, not a local intensity maximum (a peak). This is the case in numerous magic number cluster studies.<sup>19</sup> It has been shown quite clearly in the closely related systems of  $\text{NaAl}_n^-$ , studied by Nakajima and Kaya<sup>20</sup> as well as  $\text{LiAl}_n^-$  and  $\text{KAl}_n^-$ , studied by us,<sup>21</sup> where both groups found a dip, rather than a peak, in the intensity patterns at  $n=13$ . In all three of these alkali-doped aluminum cluster anions, their corresponding neutrals are 40 valence electron, closed shell species.

In addition to the peak at  $n=13$ , other persistent magic numbers were also observed at  $n=19$  and 23 in the mass spectra of  $\text{CuAl}_n^-$  cluster anions [see Figure 2(a)]. The spe-

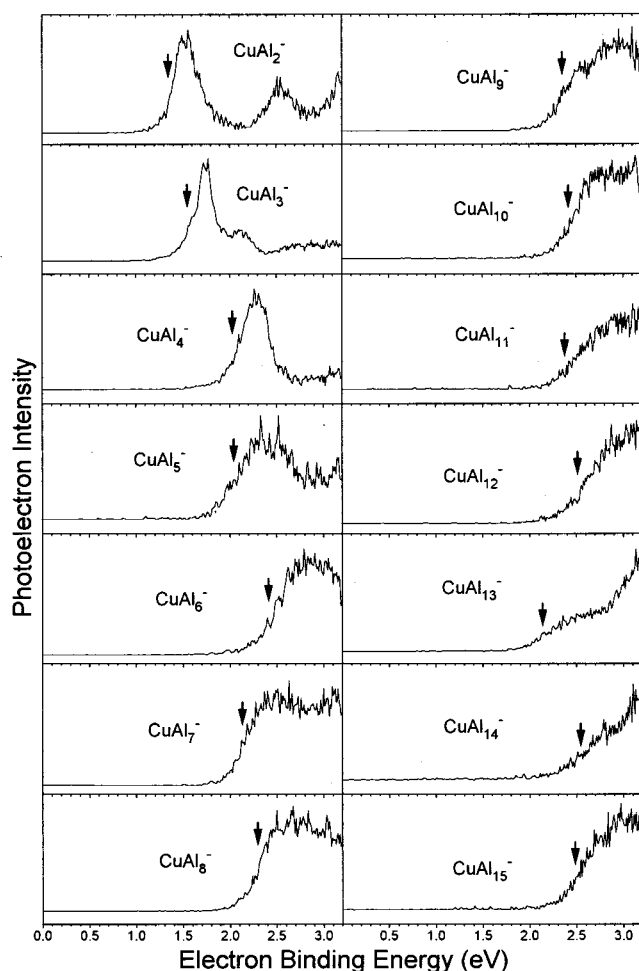


FIG. 3. Photoelectron spectra of  $\text{CuAl}_n^-$ ,  $n=2-15$ , recorded with 3.49 eV photons. The arrows indicate the locations of the origins in these spectra and thus their electron affinity values.

cies,  $\text{CuAl}_{19}^-$  and  $\text{CuAl}_{23}^-$ , however, are not peaks in the mass spectrum but appear instead as the leading elements of intensity shelves, beyond which, intensities drop abruptly to a lower level. A particularly fascinating aspect of these  $\text{CuAl}_n^-$  magic numbers is that they also correspond to those of  $\text{Al}_n^-$  cluster anions, just as if their copper atoms were absent. In studies of  $\text{Al}_n^-$  cluster anions, Castleman<sup>12</sup> has observed magic numbers at  $n=13$  and 23 in their mass spectra, and Wang<sup>15</sup> has measured spectroscopic signatures for shell closings at  $n=13$ , 19, and 23. (Our mass spectra of  $\text{Al}_n^-$  cluster anions in Fig. 2(b) also show magic numbers at  $n=13$  and 23.) These are the same magic numbers that we observe in the mass spectra of  $\text{CuAl}_n^-$ , even though  $\text{CuAl}_n^-$  cluster anions have one more atom and one more valence electron than do their respective  $\text{Al}_n^-$  counterparts. (A magic number at  $n=6$  is discussed separately below.)

### Photoelectron spectra

The photoelectron spectra of  $\text{CuAl}_n^-$ ,  $n=2-15$  are presented in Fig. 3. These spectra were recorded with 3.49 eV photons and calibrated against the transitions of the copper atomic anion. Examination of the spectra in Fig. 3 shows that they gradually shift to higher EBE's with increasing size

TABLE I. Electron affinities of  $\text{CuAl}_n^-$  versus cluster size.

Cluster size, $n$	Electron affinity (eV)
2	1.35
3	1.56
4	2.04
5	2.06
6	2.42
7	2.14
8	2.30
9	2.32
10	2.37
11	2.38
12	2.53
13	2.14
14	2.56
15	2.49

from  $n=2$  through  $n=12$ . At  $n=13$ , however, the spectrum shifts back to lower EBE by several tenths of an electron volt, only to resume its march to higher EBE's at  $n=14$  and 15. In order to make suitable intensities, the  $\text{CuAl}_n^-$  cluster anions photodetached in these spectra were generated under source conditions which did not employ helium gas in the expansion. When we measured the spectra of selected species, e.g.,  $\text{CuAl}_{13}^-$ , which had been generated with helium in the source, however, we observed essentially the same spectra, except that the low EBE tails were shifted toward higher EBE's by about a tenth of an electron volt. We assume this to be a rough measure of the extent to which hot bands may be shifting the onsets of these spectra. Taking this into account, nominal adiabatic electron affinities,  $\text{EA}_a$ , for  $\text{CuAl}_n^-$  clusters were assigned along the steeply rising portion of the low EBE side of each spectrum. These values are presented in Table I and are plotted versus size in Fig. 4, where a dip in the  $\text{EA}_a$  versus  $n$  trend at  $n=13$  and a peak at  $n=6$  are evident.

### DISCUSSION

The distilled results of this work are displayed in Figs. 2(a) and 4, these being the mass spectrum of the  $\text{CuAl}_n^-$

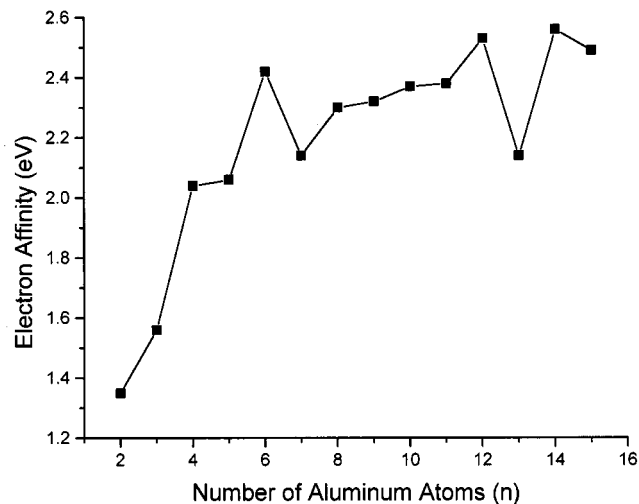


FIG. 4. Plot of measured electron affinity values for  $\text{CuAl}_n^-$  versus cluster size,  $n$ . Error bars are estimated to be  $\pm 0.1$  eV.

homologous series and the  $EA_a$  versus size behavior of  $CuAl_n$  clusters as determined from our photoelectron spectra. The mass spectrum of  $CuAl_n^-$  presents us with two closely-related questions, (1) why is the intensity of  $CuAl_{13}^-$  so high in face of conventional shell model considerations which predict it to be especially low in comparison with its immediate neighbors, and (2) why do the magic numbers for  $CuAl_n^-$  also correspond to the magic numbers for  $Al_n^-$ .

### $CuAl_{13}$ neutral clusters

The dip in the  $EA_a$  versus  $n$  trend at  $n=13$  is consistent with neutral  $CuAl_{13}$  being a closed shell species with enhanced stability. Given this stability and the fact that its anion intensity is high, the answer to the first question may be as follows. Perhaps neutral  $CuAl_{13}$  is so stable that it is also especially abundant, and the poor cross section associated with electron attachment to a closed shell species is simply overwhelmed, leading to the observed strong intensity of  $CuAl_{13}^-$  in the mass spectrum. Interpreting our results strictly in terms of conventional shell model considerations leads almost unavoidably to this conclusion, i.e., neutral  $CuAl_{13}$  must be especially stable and abundant in our source environment.

Support for the enhanced stability of neutral  $CuAl_{13}$  also comes from theory. Khanna, Jena, and Rao<sup>18</sup> found neutral  $CuAl_{13}$  to be especially stable, with an impressive gain in atomization energy of 4.42 eV over neutral  $CuAl_{12}$ . This enhanced stability is thought by these investigators to derive not only from  $CuAl_{13}$  being an electronically closed shell species, but also from its heightened geometrical stability. Their calculations revealed a  $CuAl_{13}$  structure in which the copper atom sits at the center of an icosahedral cage of 12 aluminum atoms, with the 13th aluminum atom residing on the outside. Copper is a smaller atom than aluminum, and its endohedral position leads to a relaxation of the surface strain of the cage and thus to increased geometric stabilization. Their calculated value of  $EA_a$  for  $CuAl_{13}$  is 2.17 eV, in good agreement with our measured value of 2.14 eV.

Additional support for neutral  $CuAl_{13}$  being especially stable comes from the energetic implications of our data. For clusters,  $X_n$ , the following relationship holds,

$$EA_a(X_n) - EA_a(X_{n-1}) = D(X_{n-1}^- \cdots X) - D(X_{n-1} \cdots X), \quad (2)$$

where  $EA_a(X_n)$  and  $EA_a(X_{n-1})$  denote, respectively, the electron affinities of the clusters,  $X_n$  and its smaller neighbor,  $X_{n-1}$ ,  $D(X_{n-1}^- \cdots X)$  is the dissociation energy for the loss of a single member from the cluster anion,  $X_n^-$ , and  $D(X_{n-1} \cdots X)$  is the dissociation energy for the loss of a single member of the cluster from neutral  $X_n$ . Since the  $EA_a$  of  $CuAl_{13}$  is about 0.4 eV less than that of  $CuAl_{12}$ , this implies that the energy needed to remove a single member atom from neutral  $CuAl_{13}$  is greater, by  $\sim 0.4$  eV, than the energy required to remove a single member atom from the  $CuAl_{13}^-$  cluster anion. This is an unusual inequality among clusters, where ion-neutral interaction energies are usually greater than neutral-neutral interaction energies, driving electron affinities to increase with cluster size. In the present

case, this result hints of neutral  $CuAl_{13}$  having heightened stability and provides a quantitative benchmark.

Even though neutral  $CuAl_{13}$  appears to be rather stable, it is nevertheless not evident that it is stable enough to invoke an overwhelming abundance of neutral  $CuAl_{13}$  as the sole reason for the anomalously high intensity of  $CuAl_{13}^-$  in mass spectra. Other closed shell neutral cluster species also show a dip in their  $EA_a$  versus  $n$  trends, but as anions, these species do not show local intensity maxima in their mass spectra. In fact, they usually show local minima in intensity.  $LiAl_{13}$  is an especially pertinent comparison. Not only are  $CuAl_{13}$  and  $LiAl_{13}$  stoichiometrically analogous, the difference between the  $EA_a$ 's of  $LiAl_{13}$  and  $LiAl_{12}$  is also about the same as between the  $EA_a$ 's of  $CuAl_{13}$  and  $CuAl_{12}$ . Nevertheless,  $LiAl_{13}^-$  displays a local intensity minima, not a maxima, in its mass spectrum.<sup>21</sup> The enhanced stability of neutral  $CuAl_{13}$ , while real, is not enough to explain the local intensity maximum (magic number behavior) of  $CuAl_{13}^-$  in its mass spectrum. There must be some additional reason to account for our observations.

### $CuAl_n^-$ cluster anions

Thus far, we have focused on neutral  $CuAl_{13}$ , and in doing so, we have partially answered question (1), i.e., "why is the intensity of  $CuAl_{13}^-$  so high?". We have, however, not yet dealt with question (2), i.e., "why do the magic numbers for  $CuAl_n^-$  also correspond to those of  $Al_n^-$ ?". Here, we consider the electronic structure of  $CuAl_n^-$  cluster anions in terms of the reordering of conventional (spherical) shell model energy levels. This approach adds another major component to the answer to question (1), while at the same time answering question (2) under a unified framework.

The unusual magic numbers that we observe in our mass spectra of  $CuAl_n^-$  can be explained by a jellium-like potential shape with a depression in its central region. This depression is due to high positive charge density of copper, and it represents a zone of stronger attraction for the valence electrons of the cluster. The ten  $d$  electrons in copper are relatively inefficient in shielding the copper nuclear charge of the atom. As evidence that copper has a higher effective nuclear charge than aluminum, we note that the ionization potential of a copper atom is 7.7 eV, while that of an aluminum atom is 6 eV. Copper is also a smaller atom than aluminum. Together, these facts suggest that copper should exhibit a higher positive charge density than does aluminum. The theoretical calculations of Khanna and co-workers<sup>18</sup> have found that a copper atom sits in the middle of the aluminum cage in both neutral  $CuAl_{13}$  and  $CuAl_{13}^-$  cluster anion.

The effect on the shell model energy levels of the cluster depends heavily on the probability of finding their electrons in the central region of the modified potential, where the depression is located.<sup>22,23</sup> Because of the shape of their wave functions,  $s$  levels will be affected the most, with their energies being lowered relative to higher orbital angular momenta levels. Since many levels are already close to each other in energy (especially as one climbs to higher energies), this results in a reordering of shell model energy levels, giving a new set of closed shells and thus a new set of magic

numbers. The energy ordering of spherical electronic shell levels is  $1s, 1p, 1d, 2s, 1f, 2p, 1g, 2d, 3s, 1h \dots$ , with the numbers of valence electrons needed to complete closed shells in each case being 2, 8, 18, 20, 34, 40, 58, 68, 70,  $92 \dots$ , respectively.<sup>19</sup> If, however, a  $s$ -level reordering takes place in which the  $2s$  level drops in energy to between the  $1d$  and  $1p$  levels, the  $3s$  level drops to between the  $1g$  and  $2p$  levels, and the  $4s$  level drops to between the  $1h$  and  $2d$  levels, then the numbers of valence electrons needed to complete closed shells becomes 2, 8, 10, 20, 34, 40, 42, 60, 70, and 72.

The mass spectral intensity pattern that we observe for  $\text{CuAl}_n^-$  is consistent with this reordering hypothesis, demystifying magic numbers which earlier had seemed anomalous. The magic number species shown in Fig. 2(a) are  $\text{CuAl}_{13}^-$ ,  $\text{CuAl}_{19}^-$ , and  $\text{CuAl}_{23}^-$ , these having 41, 59, and 71 valence electrons, respectively. (The magic number at  $n=6$  is discussed separately below.) While a species with one more electron than the number needed for a closed shell typically displays a local intensity minimum in its mass spectrum, a species with one less electron than is needed to fill a closed shell often exhibits a local intensity maximum, as it approaches shell closure. We have seen this quite clearly in our mass spectra<sup>21</sup> of magnesium and zinc cluster anions,  $\text{Mg}_n^-$  and  $\text{Zn}_n^-$ . While  $\text{CuAl}_{13}^-$  has one more electron than the closed shell at 40, it has just one less than the new closed shell at 42 which results from reordering.<sup>24</sup> Thus, the intensity of  $\text{CuAl}_{13}^-$ , with its 41 valence electrons, is high, in part at least, because of gathering electronic stability as it approaches the reordered closed shell at 42 electrons. Likewise, while  $\text{CuAl}_{23}^-$  has one more electron than the closed shell at 70, it has one less than the reordered closed shell at 72.  $\text{CuAl}_{19}^-$ , with its 59 valence electrons has one electron less than the reordered closed shell at 60. Thus, the magic number species,  $\text{CuAl}_{13}^-$ ,  $\text{CuAl}_{19}^-$ , and  $\text{CuAl}_{23}^-$  all have anion-oriented, electronic structure rationales for exhibiting heightened stabilities and abundances. The calculations of Khanna and co-workers,<sup>18</sup> which had found evidence for enhanced stability in neutral  $\text{CuAl}_{13}$ , also found evidence of heightened stability in  $\text{CuAl}_{13}^-$ , in agreement with the implications of reordering.

Information about the geometric structure of copper-doped aluminum cluster anions can also be inferred from these considerations. Given the assumptions of the reordering hypothesis, its success in explaining the magic number behavior of  $\text{CuAl}_{13}^-$ ,  $\text{CuAl}_{19}^-$ , and  $\text{CuAl}_{23}^-$  implies, in and of itself, that the copper atom is centrally located within these cluster anions. This is probably also true of the intervening sizes between  $n=13$  and 19 and between  $n=19$  and 23, because  $\text{CuAl}_{22}^-$  (68 valence electrons) would also be a magic number species (a closed shell, in fact) if the spherical shell model levels were being filled, and it is not. Recent calculations by Khanna and co-workers<sup>18</sup> which place the copper atom in the center of copper-doped aluminum clusters are consistent with reordering.

The correspondence between the magic numbers of  $\text{CuAl}_n^-$  and those of  $\text{Al}_n^-$  also follows naturally as a consequence of reordering, reconciling the two. The magic numbers of  $\text{Al}_n^-$  derive from spherical shell closings, while those

of  $\text{CuAl}_n^-$  arise from reordered shell closings, themselves the result of copper's perturbation of the electronic structure of aluminum cluster anions. Thus, the answer to question (2) plus a substantial part of the answer to question (1) are both consequences of reordering.

One last point about magic numbers in our mass spectra also deserves comment. Wang and co-workers<sup>15</sup> have shown that aluminum is monovalent in aluminum clusters smaller than  $\text{Al}_9$ . That implies that the species,  $\text{CuAl}_6^-$  has eight valence electrons, and by either the spherical or the reordered shell model schemes,  $\text{CuAl}_6^-$  itself should be a closed shell species. Notice that the intensity of  $\text{CuAl}_6^-$  in Fig. 2(a) is indeed a local intensity maximum relative to its immediate neighbors. The appearance of the peak at  $n=6$  in the  $\text{EA}_a$  versus  $n$  trend (see Fig. 4) is also consistent with it being designated as a closed shell, magic number species.

## CONCLUSION

Having examined the evidence relating to both neutral and anionic copper-doped aluminum clusters, we now consider the factors which govern the intensity of  $\text{CuAl}_{13}^-$  in the mass spectrum. Essentially, there are three, two of which deal with electronic stability, while the other concerns the kinetics of anion formation.  $\text{CuAl}_{13}^-$  enjoys an enhancement in stability because it is one electron short of the reordered closed shell at 42, and this is likely to result in a positive contribution to its intensity. On the other hand, because  $\text{CuAl}_{13}^-$  also has one more electron than the closed shell at 40, everything else being equal, its intensity would be expected to be weaker than its immediate neighbors. For 41 valence electron  $\text{CuAl}_{13}^-$ , the increase in its intensity due to its proximity to the closed shell at 42 and the decrease in its intensity due to the nearby closed shell at 40 are competing effects. The third factor depends on closed shell, neutral  $\text{CuAl}_{13}$  exhibiting special stability. If its stability were to translate into enough abundance, this could overwhelm the aforementioned low propensity for electrons to attach to closed shell species and contribute to the observed intensity of  $\text{CuAl}_{13}^-$ . Both anion-oriented and neutral-oriented factors may well be at work in making the  $\text{CuAl}_{13}^-$  signal what it is, but until experiments are conducted that measure the abundance of neutral  $\text{CuAl}_{13}$  in the relevant source environment, it will be difficult to dissect their relative contributions.

The goal of this work was to investigate the nature of copper-doped aluminum clusters and their anions. Evidence deriving from the photoelectron spectra and their energetic implications plus the calculations of Khanna and co-workers<sup>18</sup> imply that neutral  $\text{CuAl}_{13}$  is an unusually geometrically stable, closed electronic shell cluster with its copper atom located at the center of its aluminum cage. As for the  $\text{CuAl}_{13}^-$  cluster anion, information based on mass spectral magic numbers plus calculations by Khanna and co-workers<sup>18</sup> imply that it is an electronically and geometrically stabilized aggregate anion with a novel (reordered) electronic shell structure and a centrally located copper atom.

## ACKNOWLEDGMENTS

We thank S. N. Khanna, P. Jena, and B. K. Rao for sharing the results of their calculations with us prior to publication. This work was supported by the Division of Materials Science, Office of Basic Energy Sciences, U.S. Department of Energy under Grant No. DE-FG0295ER45538. Acknowledgment is also made to the Donors of the Petroleum Research Fund, administered by the American Chemical Society, for partial support of this research (Grant No. 28452-AC6).

- <sup>1</sup>H. W. Kroto, J. R. Heath, S. C. O'Brian, R. F. Curl, and R. E. Smalley, *Nature (London)* **318**, 162 (1985).  
<sup>2</sup>B. C. Guo, K. P. Kerns, and A. W. Castleman, Jr., *Science* **255**, 1411 (1992).  
<sup>3</sup>S. N. Khanna and P. Jena, *Phys. Rev. Lett.* **69**, 1664 (1992).  
<sup>4</sup>S. N. Khanna and P. Jena, *Phys. Rev. Lett.* **71**, 208 (1993).  
<sup>5</sup>S. N. Khanna and P. Jena, *Chem. Phys. Lett.* **218**, 383 (1994).  
<sup>6</sup>X. G. Gong and V. Kumar, *Phys. Rev. Lett.* **70**, 2078 (1993).  
<sup>7</sup>M. Manninen, J. Mansikka-aho, S. N. Khanna, and P. Jena, *Solid State Commun.* **85**, 11 (1993).  
<sup>8</sup>A. P. Seitsonen, M. J. Puska, M. Alatalo, R. M. Nieminen, V. Milman, and M. C. Payne, *Phys. Rev. Lett. B* **48**, 1981 (1993).  
<sup>9</sup>S. N. Khanna and P. Jena, *Chem. Phys. Lett.* **219**, 479 (1994).

- <sup>10</sup>S. N. Khanna and P. Jena, *Phys. Rev. B* **51**, 13705 (1995).  
<sup>11</sup>A. Rubio, L. C. Balbas, and J. A. Alonso, *Physica B* **168**, 32 (1991).  
<sup>12</sup>R. E. Leuchtner, A. C. Harms, and A. W. Castleman, Jr., *J. Chem. Phys.* **91**, 2753 (1989).  
<sup>13</sup>K. J. Taylor, C. L. Pettiette, M. J. Craycroft, O. Chesnovsky, and R. E. Smalley, *Chem. Phys. Lett.* **152**, 347 (1988).  
<sup>14</sup>G. Gantefoer, M. Gausa, K. H. Meiwes-Broer, and H. O. Lutz, *Faraday Discuss. Chem. Soc.* **86**, 197 (1988).  
<sup>15</sup>X. Li, H. Wu, X.-B. Wang, and L.-S. Wang, *Phys. Rev. Lett.* **81**, 1909 (1998).  
<sup>16</sup>K. J. Taylor, C. L. Pettiette-Hall, O. Chesnovsky, and R. E. Smalley, *J. Chem. Phys.* **96**, 3319 (1992).  
<sup>17</sup>C.-Y. Cha, G. Gantefoer, and W. Eberhardt, *J. Chem. Phys.* **99**, 6308 (1993).  
<sup>18</sup>S. N. Khanna, P. Jena, and B. K. Rao (private communication).  
<sup>19</sup>W. D. Knight, K. Clemenger, W. A. de Heer, W. A. Saunders, M. Y. Chou, and M. L. Cohen, *Phys. Rev. Lett.* **52**, 2141 (1984).  
<sup>20</sup>A. Nakajima, K. Hoshino, T. Sugioka, T. Naganuma, T. Taguwa, Y. Yamada, K. Watanabe, and K. Kaya, *J. Phys. Chem.* **97**, 86 (1993).  
<sup>21</sup>O. C. Thomas, W. Zheng, and K. H. Bowen, Jr. (unpublished).  
<sup>22</sup>W. D. Knight, W. A. de Heer, W. A. Saunders, and K. Clemenger, *Chem. Phys. Lett.* **134**, 1 (1987).  
<sup>23</sup>C. Baladron and J. A. Alonso, *Physica B* **154**, 73 (1988).  
<sup>24</sup>The conclusion that the dip in the  $EA_n$  versus  $n$  trend at  $n=13$  is indicative of neutral  $CuAl_{13}$  being a closed shell species remains valid, since 40 is also a magic number under reordering.